

## **Master's Thesis**

# **Coil Array Inductive Power Transfer System for Autonomous Underwater Vehicle**

Yu Cheng

Program of Information Science and Engineering  
Graduate School of Information Science  
Nara Institute of Science and Technology

Supervisor: Professor Minoru Okada  
Network Systems Lab. (Division of Information Science)

January 18, 2021

A Master's Thesis  
submitted to Graduate School of Information Science,  
Nara Institute of Science and Technology  
in partial fulfillment of the requirements for the degree of  
Doctor of ENGINEERING

Yu Cheng

Thesis Committee:

Professor Minoru Okada

(Supervisor, Division of Information Science)

Professor Yuichi Hayashi

(Co-supervisor, Division of Information Science)

Associate Professor Takeshi Higashino

(Co-supervisor, Division of Information Science)

Assistant Professor Quang-Thang Duong

(Co-supervisor, Division of Information Science)

Assistant Professor Na Chen

(Co-supervisor, Division of Information Science)

# **Coil Array Inductive Power Transfer System for Autonomous Underwater Vehicle\***

Yu Cheng

## **Abstract**

For a long time, providing a stable, safe, and efficient power supply for underwater electromechanical equipment has always been a concern in deep-sea exploration. Compared with the complicated docking mechanism, potential safety hazards, and expensive price of traditional wet-mate connectors, wireless power transmission (WPT) technology can transmit energy without any electrical contact between the power supply and the electrical equipment, which provides an effective solution to the aforementioned drawbacks of wired charging. There are many uncontrollable factors in the seawater working environment. Therefore, this topic takes the equivalent circuit and magnetic field distribution as the theoretical basis to study the energy transmission characteristics of underwater WPT and proposes corresponding improvements and solutions to the current problems and deficiencies. Especially for the unstable output voltage of the receiver and excessive magnetic flux density at the internal of AUV.

## **Keywords:**

Autonomous underwater vehicle, inductive power transfer, underwater wireless power transfer, undersea

---

\*Master's Thesis, Graduate School of Science and Technology, Nara Institute of Science and Technology, January 18, 2021.

# Contents

|   |           |
|---|-----------|
| <b>List of Figures</b>                                    | <b>iv</b> |
| <b>List of Tables</b>                                     | <b>v</b>  |
| <b>1 Introduction</b>                                     | <b>1</b>  |
| 1.1 Background and research purpose . . . . .             | 1         |
| 1.2 Wireless power transfer technologies . . . . .        | 3         |
| 1.3 Underwater wireless power transfer . . . . .          | 4         |
| 1.3.1 Underwater environment . . . . .                    | 5         |
| 1.3.2 Common UWPT systems . . . . .                       | 6         |
| 1.4 The main research content of this thesis . . . . .    | 6         |
| 1.5 Roadmap . . . . .                                     | 7         |
| <b>2 Basic principles of IPT</b>                          | <b>8</b>  |
| 2.1 Inductive coupling model . . . . .                    | 8         |
| 2.2 Compensation network technologies . . . . .           | 9         |
| 2.2.1 S-S compensation topology . . . . .                 | 10        |
| 2.2.2 CLC-S compensation topology . . . . .               | 11        |
| 2.3 Underwater WPT system model . . . . .                 | 12        |
| <b>3 Preliminary exploration of underwater IPT system</b> | <b>13</b> |
| 3.1 The system in three different media . . . . .         | 13        |
| 3.2 The system in different distance . . . . .            | 14        |
| 3.3 The system in different frequency . . . . .           | 17        |
| 3.4 Conclusion . . . . .                                  | 17        |

|   |           |
|---|-----------|
| <b>4 Coil array WPT</b>                     | <b>19</b> |
| 4.1 Simulation evaluation . . . . .         | 25        |
| 4.1.1 Simulation evaluation . . . . .       | 25        |
| 4.2 Coil array WPT in the air . . . . .     | 25        |
| 4.3 Coil array WPT under seawater . . . . . | 25        |
| <b>5 Conclusion</b>                         | <b>26</b> |
| 5.1 Future works . . . . .                  | 26        |
| <b>References</b>                           | <b>28</b> |

# List of Figures

|      |   |    |
|------|---|----|
| 1.1  | Underwater sensor networks architecture [2]. . . . .                    | 2  |
| 1.2  | Near-field wireless power transfer. . . . .                             | 4  |
| 1.3  | Far-field wireless power transfer. . . . .                              | 5  |
| 1.4  | Stacked UWPT system [4]. . . . .  | 6  |
| 1.5  | Plug-in UWPT system [5]. . . . .  | 6  |
| 2.1  | Inductive coupling model. . . . .                                       | 8  |
| 2.2  | Equivalent circuit of inductive coupling model. . . . .                 | 9  |
| 2.3  | Compensation networks. . . . .  | 10 |
| 2.4  | S-S structure. . . . .  | 11 |
| 2.5  | CLC-S structure. . . . .  | 12 |
| 3.1  | Two ring structure. . . . .   | 13 |
| 3.2  | Two ring structure ( $r_{inner} = 50mm$ , $r_{outer} = 80mm$ ). . . . . | 15 |
| 4.1  | Underwater sensor networks architecture. . . . .                        | 19 |
| 4.2  | Underwater sensor networks architecture. . . . .                        | 20 |
| 4.3  | Two ring structure. . . . .   | 20 |
| 4.4  | Coil-array IPT structure. . . . .                                       | 21 |
| 4.5  | Coil-array IPT structure. . . . .                                       | 21 |
| 4.6  | Coil-array IPT structure. . . . .                                       | 22 |
| 4.7  | Coil-array IPT structure. . . . .                                       | 22 |
| 4.8  | Coil-array IPT structure. . . . .                                       | 23 |
| 4.9  | Coil-array IPT structure. . . . .                                       | 23 |
| 4.10 | Coil-array IPT structure. . . . .                                       | 24 |
| 4.11 | Coil-array IPT structure. . . . .                                       | 24 |

# List of Tables

|     |  |    |
|-----|--|----|
| 1.1 | The different wireless power transmission technologies. . . . .                      | 3  |
| 2.1 | The dielectric constant & conductivity of some materials at 25°C under 1kHz. . . . . | 12 |
| 3.1 | The parameters of ring coil structure. . . . .                                       | 14 |
| 3.2 | The parameters of ring coil structure. . . . .                                       | 15 |
| 3.3 | Z-parameters in different distance and media . . . . .                               | 16 |
| 3.4 | The parameters of ring coil structure. . . . .                                       | 17 |
| 3.5 | Z-parameters in different frequencies and media . . . . .                            | 18 |
| 4.1 | Maximum power transfer efficiency. . . . .   | 25 |

# 1 Introduction

## 1.1 Background and research purpose

In the foreseeable future, the electrification of ocean systems, renewable ocean power sources, and ocean energy networks will be necessary, which will help accelerate the growth and deployment of ocean renewable energy and ways to explore and understand the ocean [1]. To achieve electrification in the ocean, it is necessary to deploy corresponding sensor networks underwater and process the data received by underwater sensors in a timely manner (Figure 1.1). At the same time, underwater sensors are also an essential tool for studying the marine environment. They can easily and flexibly explore underwater terrain and ecological environment, which provides convenience for the deployment of underwater sensor networks. An excellent underwater AUV needs to have good equipment waterproofness, long-distance underwater controllability, and power durability. For the water-resistance of the equipment, we can use high-performance waterproof and pressure-resistant materials. The remote controllability needs to solve the problems of long-distance underwater wireless communication. The durability of electrical equipment requires low energy consumption AUV and high-energy batteries or a continuous power supply. Sufficient power supply can keep underwater sensors and AUVs in an efficient and stable working state for a long time. Indirectly, reducing human interference when electrical equipment is working underwater can also improve work efficiency and reduce deployment costs. Therefore, the energy supply for underwater electrical equipment has become a novel research direction. Such methods can solve the energy supply problem of underwater equipment economically and ensure the system to perform long-term and stable work [3].

In traditional marine engineering, power is supplied to underwater equipment

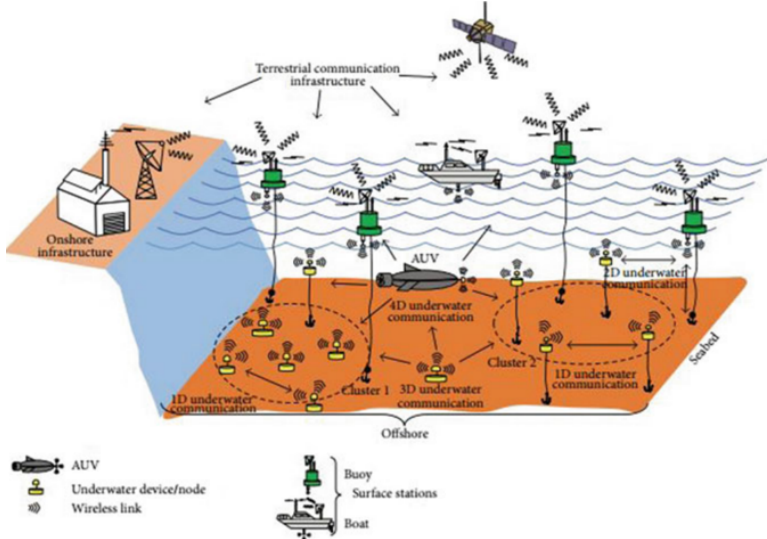


Figure 1.1: Underwater sensor networks architecture [2].

through wet-mate subsea connectors [4]. For the traditional wet plug interface technology, its high cost, complex docking method, poor safety performance, and easy to be corroded by seawater, make its disadvantages in marine engineering increasingly obvious. Wireless Power Transfer (WPT) simplifies the connection between underwater equipment and power supply, reduces the continuous operating cost of underwater equipment, saves a lot of resources, and gradually gains the favor of scholars.

The ocean itself and its surroundings contain a lot of energy, such as tidal energy, wave energy, ocean current energy, sea temperature difference energy, and sea salt difference energy. Ocean energy is rich, widely distributed, clean, and pollution-free, but low energy density and strong regionality. These advantages make it attractive as grid-connected energy, and may also make it an isolated and remote ocean energy source, thereby providing a valuable source of ocean space. Continuous development provides power solutions that are attractive. The rapid development of distributed ocean energy applications (such as underwater sensor networks, ocean sensors and monitoring technologies, ocean automatic network buoys, and deep-sea and tsunami buoys) is beneficial. In particular, it can power an autonomous underwater vehicle (AUV) whose service life is limited by its battery power.

## 1.2 Wireless power transfer technologies

Broadly speaking, power transfer without direct electrical contact between the primary and secondary is wireless power transfer. Wireless power technology can be divided into two main categories, near-field (nonradiative region) power transfer and far-field (radiative region) power transfer. Near-field means the area within about 1 wavelength ( $\lambda$ ) of the antenna. The range of near-field devices is conventionally divided into two categories [ref] (Suppose the distance between two antennas is represented by  $D_{range}$ , and the diameter of two antenna coils is represented by  $D_{ant.}$ ):

- Short range, the distance between two antennas is less than the diameter of antenna:  $D_{range} \leq D_{ant.}$ . In this range, power is usually transferred through non-resonant capacitive or inductive coupling.
- Mid-range, the distance between two antennas is less than 10 times the diameter of antenna:  $D_{range} \leq 10D_{ant.}$ . In this range, energy is usually transferred through resonant capacitive or inductive coupling.

Table 1.1: The different wireless power transmission technologies.

| Technology | Range    | Frequency  | Antenna devices                                   | Applications   |
|------------|----------|------------|---|--|
| Microwaves | hm – km  | GHz        | Parabolic dishes,<br>phased arrays,<br>rectennas  | Satellite, drone<br>aircraft                               |
| Optical    | dam – km | $\geq$ THz | Lasers, photocells,<br>lenses                     | Drone aircraft,<br>space elevator                          |
| Capacitive | cm – m   | kHz – MHz  | Metal plate<br>electrodes                         | Smartcards,<br>biomedical implant                          |
| Inductive  | mm – m   | Hz – GHz   | Tuned wire coils,<br>lumped element<br>resonators | Electric<br>toothbrush,<br>smartphone,<br>electric vehicle |

Far-field or radiative region, power is transmitted by means of electromagnetic

waves, like radio waves, microwaves, or light waves. When the operating frequency ( $f$ ) is relatively low, wavelength  $\lambda = c/f$ , at this time the diameter of the antenna is much smaller than the wavelength,  $D_{ant} \ll \lambda$ , and the radiated power will be very small. When the diameter of antenna is about wavelength,  $D_{ant} \approx \lambda$ , radiate power will be efficient. When the diameter of antenna is much greater than wavelength,  $D_{ant} \gg \lambda$ , we can use high-gain antennas to concentrate electromagnetic waves on a narrow beam and directly aim at the receiver to improve transmission efficiency.

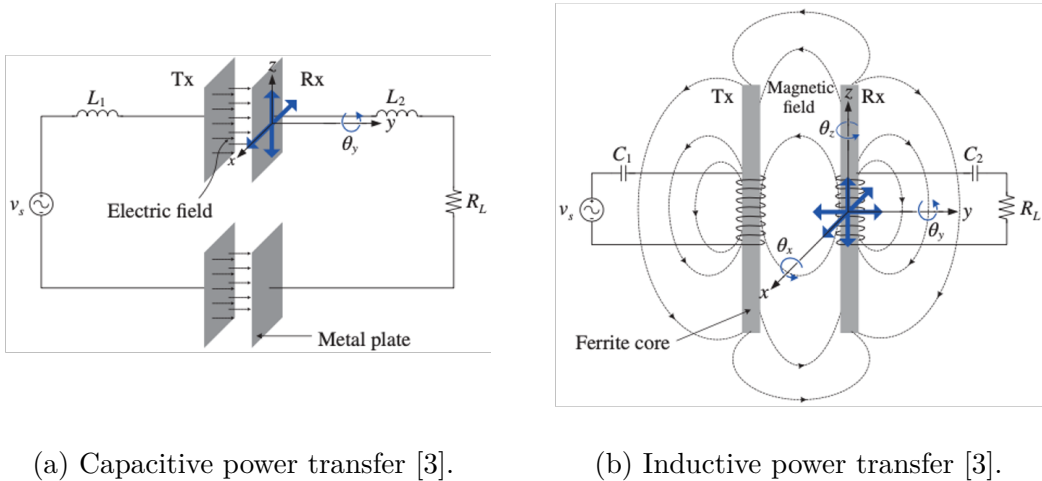
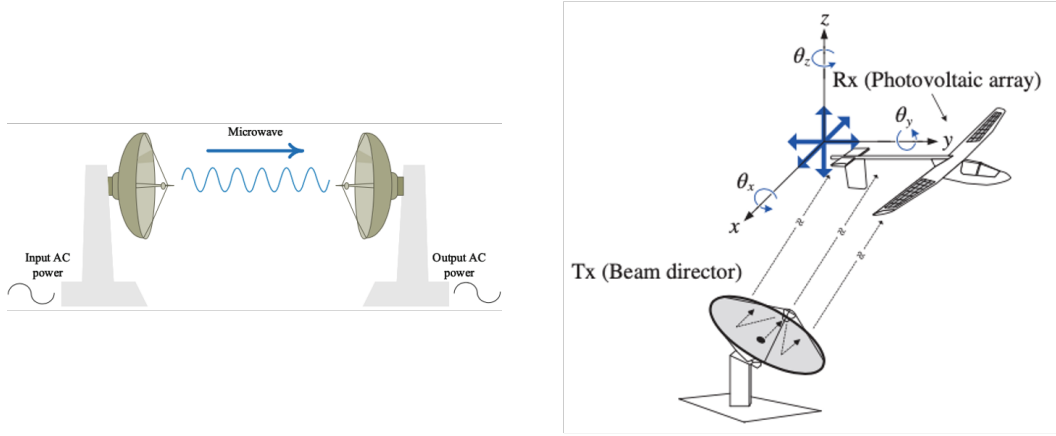


Figure 1.2: Near-field wireless power transfer.

Therefore, near-field wireless power transfer systems mainly include inductive coupling power transfer and capacitive coupling power transfer (Figure 1.2). Far-field wireless power transfer systems mainly include microwave, optical, and acoustic power transfer (Figure 1.3). The respective characteristics are shown in the table 1.1.

### 1.3 Underwater wireless power transfer

WPT technology has unique advantages in special environments, and along with the continuous development of landing application research and the emergence of a large number of results, it has attracted the attention of underwater technology



(a) Microwave power transfer [1].

(b) Laser power transfer [3].

Figure 1.3: Far-field wireless power transfer.

researchers.

### 1.3.1 Underwater environment

Underwater, Seawater has a blocking effect on high-frequency electromagnetic waves. The distance of electromagnetic waves propagating underwater is inversely proportional to the frequency, making it difficult to achieve long-distance power transmission.

**Conductivity:** Due to the electrical conductivity of seawater, traditional wireless power transmission analysis methods are no longer applicable. At present, the system modeling and related theoretical analysis of underwater wireless power transfer technology need to be improved.

**Undercurrent:** The submarine landform is complex and there is undercurrent. The coupler core is liable to drift under water, and there are problems such as difficulty in docking, which results in low transmission efficiency.

**Other Impact:** Microbial enrichment, temperature, salinity

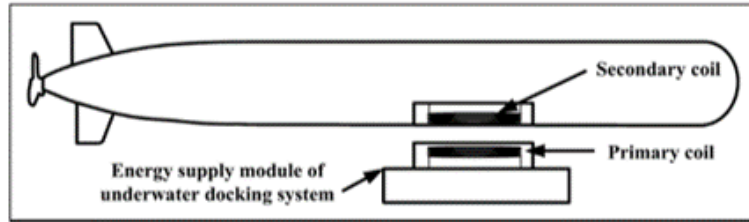


Figure 1.4: Stacked UWPT system [4].

### 1.3.2 Common UWPT systems

Saddle structure transmitter Easy parking, but the receiver is easy to shift when charging

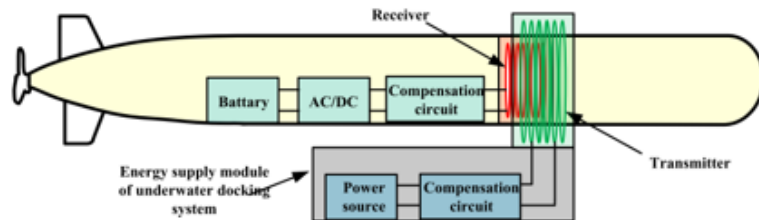


Figure 1.5: Plug-in UWPT system [5].

Hollow cylindrical structure transmitter Difficult parking, the receiver is not easy to shift when charging

## 1.4 The main research content of this thesis

This paper mainly studies the underwater wireless power transfer system, and analyzes the difference between the underwater environment and the land environment WPT system. Considering the durability and high reliability of underwater AUV, this paper proposes a novel coil array power transfer system. It provides reference materials for the subsequent research on the wpt system of multiple coil groups.

## 1.5 Roadmap

The first chapter analyzes the background of this research and its research purpose and significance, analyzes the characteristics and advantages and disadvantages of mainstream WPT technology, and provides a basis for using IPT technology as an underwater wireless energy transmission system in the following text. A detailed summary and analysis of the current research status of related technologies at home and abroad, including underwater wired energy transmission technology, WPT technology in underwater and air media, and an explanation of the research focus of this article.

The second chapter focuses on the analysis of the basic theory of wireless energy transmission. First, the basic IPT model is explained, and its working principle is analyzed. Then explained the related technology of compensation network. Finally, analyze the underwater IPT system model.

## 2 Basic principles of IPT

This chapter will first introduce the principle of IPT technology from the physical level, and then introduce the principle of IPT technology from the circuit level, analyze the relationship between different equivalent models, and derive system energy transmission indicators that can represent system performance. And analyze the influence of relevant design parameters on system transmission performance. Analyze the influence of the medium on the system performance in the WPT process, and propose an equivalent model in the underwater working environment. Perform simulation analysis on the derivation to ensure that complete theoretical support is provided for more detailed theoretical research and research on new IPT technology.

### 2.1 Inductive coupling model

Figure 2.1 depicts the circuit model of IPT systems, where the transmitting coil L<sub>1</sub> and the receiving coil L<sub>2</sub> are directly connected to the power source and the load, respectively. Denote M as the mutual inductance, r<sub>1</sub> and r<sub>2</sub> as the equivalent AC resistance of coils.

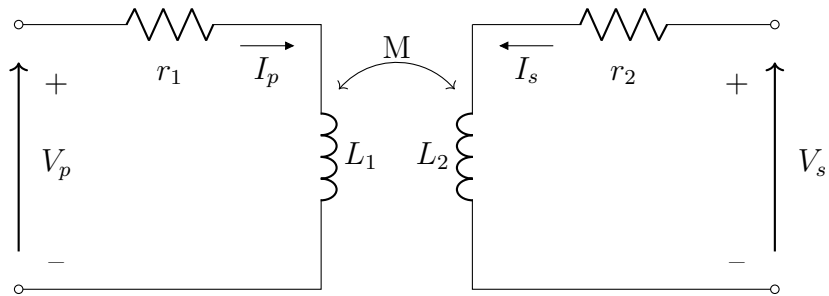


Figure 2.1: Inductive coupling model.

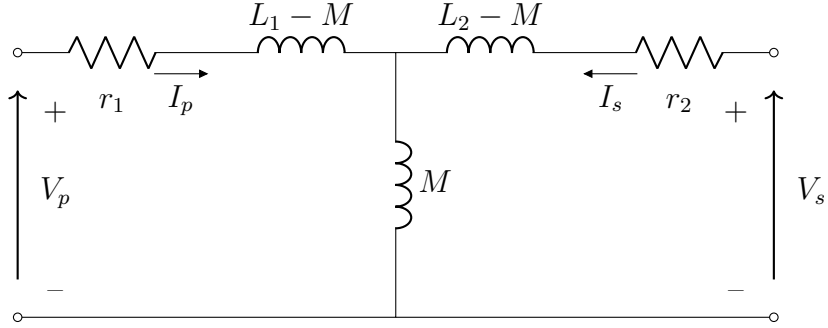


Figure 2.2: Equivalent circuit of inductive coupling model.

Therefore, the equivalent circuit can be expressed as figure 2.2. According to the Kirchhoff's circuit laws. The following formulas can be easily found.

$$V_p = I_p[r_1 + j\omega(L_1 - M)] + (I_p + I_s)j\omega M \quad (2.1)$$

$$= r_1 I_p + j\omega L_1 I_p - j\omega M I_p + j\omega M I_p + j\omega M I_s \quad (2.2)$$

$$= (r_1 + j\omega L_1) I_p + j\omega M I_s \quad (2.3)$$

$$V_s = j\omega M I_p + (r_2 + j\omega L_2) I_s \quad (2.4)$$

The above equations can be expressed as the following matrix equation.

$$\begin{bmatrix} V_p \\ V_s \end{bmatrix} = \begin{bmatrix} r_1 + j\omega L_1 & j\omega M \\ j\omega M & r_2 + j\omega L_2 \end{bmatrix} \begin{bmatrix} I_p \\ I_s \end{bmatrix} \quad (2.5)$$

If we use  $\mathbf{V}$ ,  $\mathbf{Z}$ ,  $\mathbf{I}$  to express the corresponding matrices. The formula 2.5 can be represented as follows.

$$\mathbf{V} = \mathbf{Z} \cdot \mathbf{I} \quad (2.6)$$

Here, the imaginary part of  $Z_{11}$  ( $j\omega L_1$ ) and  $Z_{22}$  ( $j\omega L_2$ ) can be canceled by the compensation networks.

## 2.2 Compensation network technologies

A compensation network is a network that makes some adjustments to compensate for system electrical defects. If capacitor compensation is used only on the

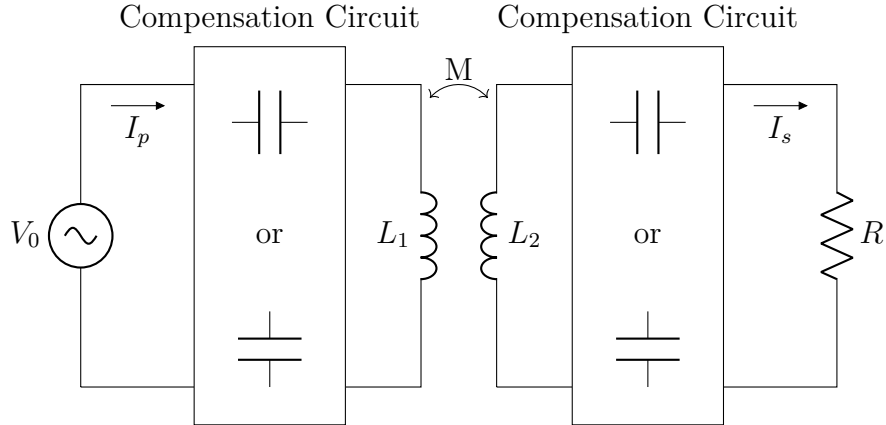


Figure 2.3: Compensation networks.

primary or secondary side, it is called single-sided compensation topology; when capacitor compensation is used on both the primary and secondary sides at the same time, it is called double-sided compensation topology. The calculation of the capacitance value of single-sided compensation is relatively simple, but the actual effect is not as good as the double-sided compensation method. Therefore, this article only discusses bilateral compensation. As shown in the figure 2.3, according to the different connection modes of the capacitors on both sides, common resonance compensation technologies can be divided into four structures: S-S, S-P, P-S, P-P (S: series, P: parallel). In addition, there are more complicated compensation networks such as CLC and LCC.

Since only S-S topology and CLC-S topology are used in the following text, we only analyze these two compensation topologies in detail here.

### 2.2.1 S-S compensation topology

When the inductors and the capacitors in the resonance state, we have,

$$\omega = \omega_0 = \frac{1}{\sqrt{LC}} \quad (2.7)$$

where  $\omega$  represents the working frequency,  $\omega_0$  represents the resonant angular frequency of the circuit. Here, to maximize the transmission efficiency of the WPT system, we need to make the resonant frequencies of the primary side and

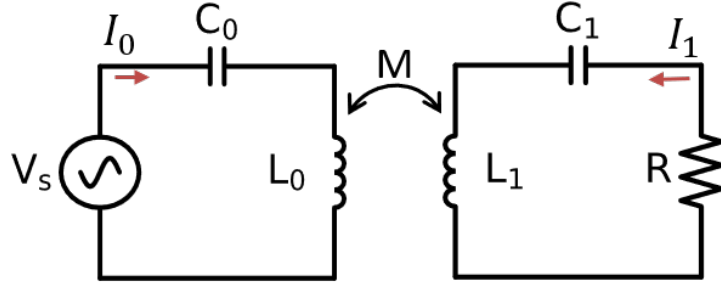


Figure 2.4: S-S structure.

secondary side consistent. Therefore,

$$\omega_0 = \frac{1}{L_1 C_1} = \frac{1}{L_2 C_2} \quad (2.8)$$

For any formed coil, we can measure its corresponding inductance value at a specified frequency. Thus, we can get the value of the compensation capacitor by formula 2.7.

$$C = \frac{1}{\omega_0^2 L} \quad (2.9)$$

$$k = \frac{M}{\sqrt{L_1 L_2}} \quad (2.10)$$

### 2.2.2 CLC-S compensation topology

$$V_S = -jX_C I_S + jX_L I_L \quad (2.11)$$

$$V_0 = (-jX_{C_0} + jX_{L_0} + r_0)I_0 + j\omega M I_1 \quad (2.12)$$

$$V_R = j\omega I_0 + (-jX_{C_1} + jX_{L_1} + r_1)I_1 \quad (2.13)$$

$$V_R = -RI_1 \quad (2.14)$$

$$I_S = I_L + I_0 \quad (2.15)$$

$$V_R = -\frac{R}{R+r_1} \cdot \frac{\omega M}{X_L} V_S \quad (2.16)$$

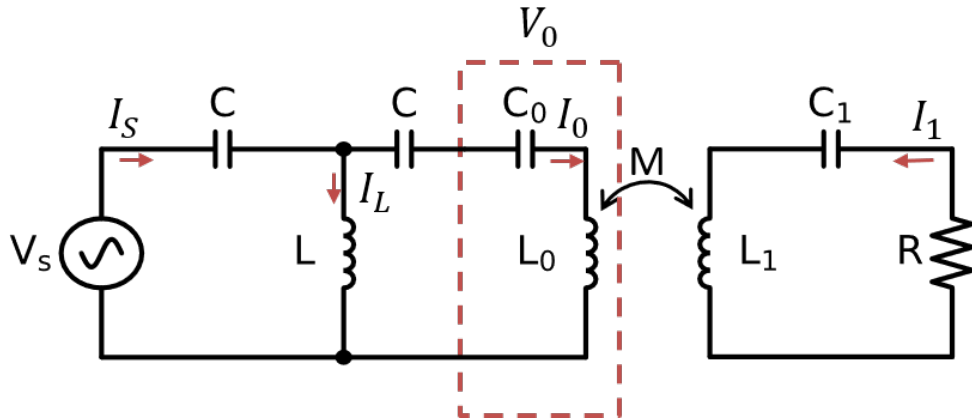


Figure 2.5: CLC-S structure.

## 2.3 Underwater WPT system model

In the seawater environment, the electrical parameters of seawater as the transmission medium are quite different from those in the air, as shown in the table. Therefore, the conventional mutual inductance model of Eq. and Eq. cannot reflect the influence of seawater media on transmission, and cannot completely and accurately describe the transmission behavior under seawater.

Table 2.1: The dielectric constant & conductivity of some materials at 25°C under 1kHz.

| Material         | Relative permittivity | Conductivity             |
|------------------|-----------------------|--------------------------|
| Vacuum           | 1                     | 0 S/m                    |
| Air              | 1.0006                | 0 S/m                    |
| Ultra pure water | 81                    | $5.5 \times 10^{-6}$ S/m |
| Drinking water   | 81                    | 0.005 – 0.05 S/m         |
| Seawater         | 81                    | 5 S/m                    |

### 3 Preliminary exploration of underwater IPT system

In order to explore the similarities and differences between the wireless energy transmission system in the seawater environment and the wireless energy transmission system in the air in the actual situation, a simple double-coil structure is used to explore the electrical properties of the underwater environment. This chapter will introduce the performance of the double coil structure working in sea water.

#### 3.1 The system in three different media



(a) Experimental coil.



(b) Structure diagram.

Figure 3.1: Two ring structure.

In order to design a wireless power transmission system suitable for underwater AUV, we will first use hollow cylindrical structure transmitter and cylindrical

structure receiver to explore the performance of the UWPT system of this plug-in structure UWPT in water. For the convenience of writing, it will be referred to as a double ring structure in the following text. The coil structure as shown in figure 4.3.

Its detailed parameters are shown in Table 3.1.

Table 3.1: The parameters of ring coil structure.

| Items                             | Parameters               |
|-----------------------------------|--------------------------|
| Environment                       | Air, tap water, seawater |
| Wire diameter                     | 0.8mm                    |
| Wire material                     | Copper                   |
| Tx coil diameter                  | 113mm                    |
| Rx coil diameter                  | 85mm                     |
| Turns (Inner coil and outer coil) | 10                       |
| Frequency                         | 200kHz                   |

When we use the VNA analyzer to place the coil in the air, tap water, or sea water for measurement, the following data can be obtained:

$$Z_{Air} = \begin{bmatrix} 0.4 + 29.6i & 0.0 - 10.0i \\ 0.0 - 10.0i & 0.3 + 20.3i \end{bmatrix},$$

$$Z_{Tap-water} = \begin{bmatrix} 3.0 + 32.1i & -1.5 - 11.3i \\ -1.5 - 11.3i & 1.5 + 21.6i \end{bmatrix},$$

$$Z_{Seawater} = \begin{bmatrix} 7.2 + 37.8i & -6.0 - 15.7i \\ -6.0 - 15.7i & 6.5 + 25.3i \end{bmatrix}.$$

In the above measurement results, we can find that as the transmission medium changes (Air to tap-water to seawater), each corresponding value is increasing.

## 3.2 The system in different distance

In order to explore the influence of the size of the internal coil and the distance between the two coils on the system (Figure 3.2), the coil size is changed here

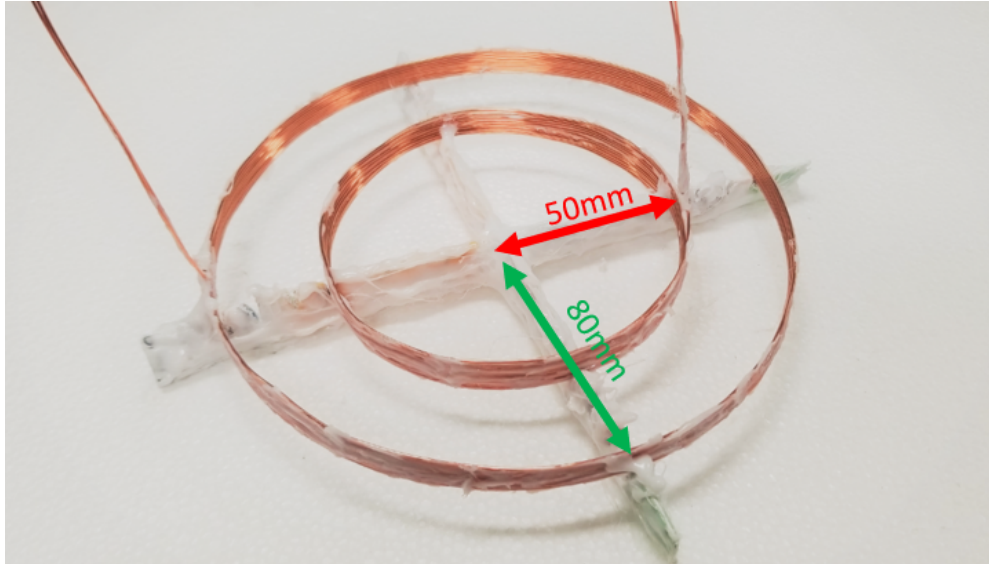


Figure 3.2: Two ring structure ( $r_{inner} = 50\text{mm}$ ,  $r_{outer} = 80\text{mm}$ ).

to change the distance between the transmitter and the receiver. The specific parameters are as follows (Table 3.2).

Table 3.2: The parameters of ring coil structure.

| Items                             | Parameters               |
|-----------------------------------|--------------------------|
| Environment                       | Air, tap water, seawater |
| Wire diameter                     | 0.8mm                    |
| Wire material                     | Copper                   |
| Tx coil diameter                  | 160mm                    |
| Rx coil diameter                  | 100mm, 120mm, 140mm      |
| Turns (Inner coil and outer coil) | 10                       |
| Frequency                         | 200kHz                   |

After changing the medium between the coils and the distance between the coils, the Z-parameters in different scenarios are measured by VNA, and we get the following results (Table 3.3).

Table 3.3: Z-parameters in different distance and media

| Media     | Coil size (Radius) | Distance | Z-parameter          |                      |
|-----------|--------------------|----------|----------------------|----------------------|
| Air       | 80mm - 50mm        | 30mm     | $0.6826 + 46.4075i$  | $-0.0411 - 8.9620i$  |
|           | 80mm - 60mm        | 20mm     | $-0.0382 - 8.9669i$  | $0.3423 + 24.2260i$  |
|           | 80mm - 70mm        | 10mm     | $0.7194 + 46.1416i$  | $-0.0946 - 15.0048i$ |
| Tap-water | 80mm - 50mm        | 20mm     | $-0.0906 - 15.0155i$ | $0.5225 + 32.5246i$  |
|           | 80mm - 60mm        | 10mm     | $0.6657 + 45.9561i$  | $0.0757 + 24.2562i$  |
|           | 80mm - 70mm        | 30mm     | $0.0699 + 24.2747i$  | $0.5651 + 39.2948i$  |
| Seawater  | 80mm - 50mm        | 30mm     | $5.4603 + 53.0814i$  | $-2.4332 - 11.7753i$ |
|           | 80mm - 60mm        | 20mm     | $-2.4304 - 11.7859i$ | $1.7722 + 26.0449i$  |
|           | 80mm - 70mm        | 10mm     | $7.0513 + 54.2993i$  | $-4.4889 - 20.1926i$ |
|           | 80mm - 50mm        | 20mm     | $-4.4867 - 20.2100i$ | $3.9114 + 36.7652i$  |
|           | 80mm - 60mm        | 10mm     | $2.8768 + 49.8765i$  | $0.9991 + 26.5644i$  |
|           | 80mm - 70mm        | 30mm     | $0.9946 + 26.5864i$  | $1.9865 + 42.0751i$  |

### **3.3 The system in different frequency**

Earlier we have studied the z-parameter changes of the two ring coil structure under different media and different distances. In this section we will study how z-parameters changes at different frequencies. Table 3.4 a shows the parameters of the experiment.

Table 3.4: The parameters of ring coil structure.

| Items                             | Parameters                             |
|-----------------------------------|--|
| Environment                       | Air, seawater                          |
| Wire diameter                     | 0.8mm                                  |
| Wire material                     | Copper                                 |
| Tx coil diameter                  | 160mm                                  |
| Rx coil diameter                  | 100mm                                  |
| Turns (Inner coil and outer coil) | 10                                     |
| Frequency                         | 100kHz, 150kHz, 200kHz, 250kHz, 300kHz |

After using the above parameters, we got the following results (Table 3.3).

### **3.4 Conclusion**

Table 3.5: Z-parameters in different frequencies and media

| Media    | Frequency | Z-parameter          |                      |                     |
|----------|-----------|----------------------|----------------------|---------------------|
| Air      | 100kHz    | $0.3758 + 23.2130i$  | $-0.0036 - 4.4495i$  |                     |
|          |           | $-0.0012 - 4.4520i$  | $0.2123 + 12.1526i$  |                     |
|          | 150kHz    | $0.4789 + 34.7320i$  | $-0.0074 - 6.6739i$  |                     |
|          |           | $-0.0037 - 6.6774i$  | $0.2575 + 18.1971i$  |                     |
|          | 200kHz    | $0.5755 + 46.2288i$  | $-0.0121 - 8.9004i$  |                     |
|          |           | $-0.0050 - 8.9065i$  | $0.3031 + 24.2211i$  |                     |
| Seawater | 250kHz    | $0.6737 + 57.7432i$  | $-0.0153 - 11.1342i$ |                     |
|          |           | $-0.0095 - 11.1426i$ | $0.3423 + 30.2465i$  |                     |
|          | 300kHz    | $0.7556 + 69.2691i$  | $-0.0191 - 13.3746i$ |                     |
|          |           | $-0.0100 - 13.3859i$ | $0.3791 + 36.2676i$  |                     |
|          | 100kHz    | $0.5314 + 24.3255i$  | $-0.0760 - 4.9832i$  |                     |
|          |           | $-0.0717 - 4.9862i$  | $0.2593 + 12.5247i$  |                     |
|          | 150kHz    | $0.9900 + 39.2700i$  | $-0.2453 - 8.8345i$  |                     |
|          |           | $-0.2392 - 8.8400i$  | $0.4080 + 19.6434i$  |                     |
|          | 200kHz    | $2.0236 + 59.0193i$  | $-0.7053 - 15.0451i$ |                     |
|          |           | $-0.6942 - 15.0581i$ | $0.7248 + 28.1895i$  |                     |
|          | 250kHz    | $4.8486 + 89.4034i$  | $-2.0763 - 26.6084i$ |                     |
|          |           | $-2.0597 - 26.6276i$ | $1.5345 + 39.8440i$  |                     |
|          | 300kHz    | $1.0e + 02 *$        | $0.1548 + 1.4909i$   | $-0.0751 - 0.5327i$ |
|          |           |                      | $-0.0749 - 0.5333i$  | $0.0450 + 0.5985i$  |

## 4 Coil array WPT

Through the explanation in the previous chapter, we know the basic performance of the wireless transmission system underwater. This chapter will introduce the underwater coil group wpt system we designed, by degrading a large double coil structure into multiple small coil structures. This greatly reduces the magnetic field in the internal coil, thereby achieving electromagnetic protection inside the AUV system.

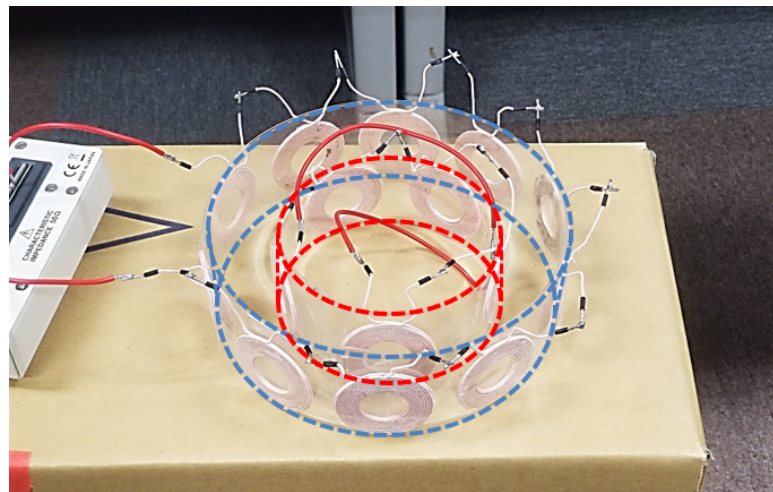


Figure 4.1: Underwater sensor networks architecture.

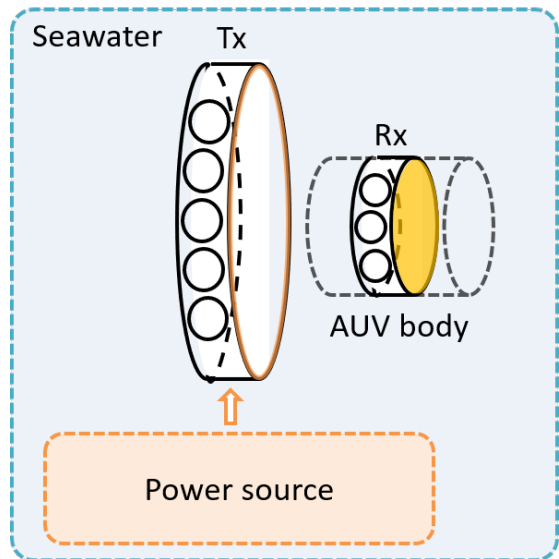
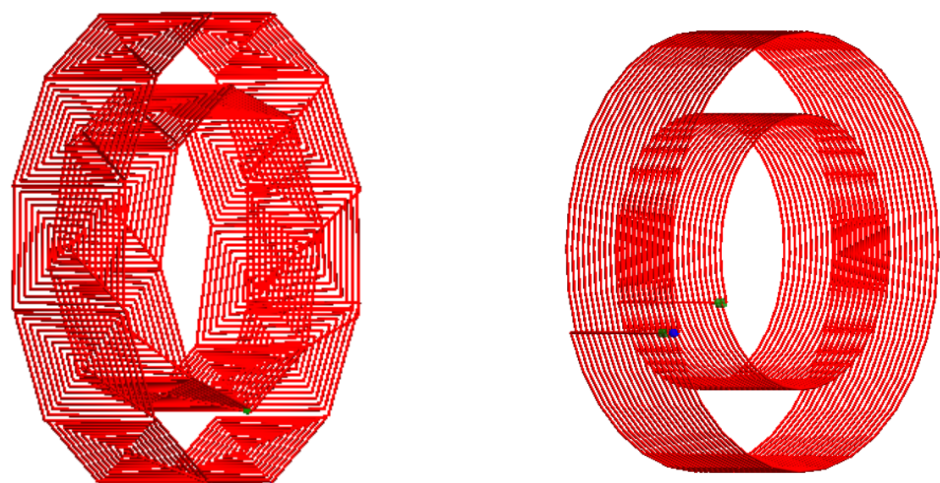


Figure 4.2: Underwater sensor networks architecture.



(a) Coil-array IPT structure.

(b) Two ring IPT structure.

Figure 4.3: Two ring structure.

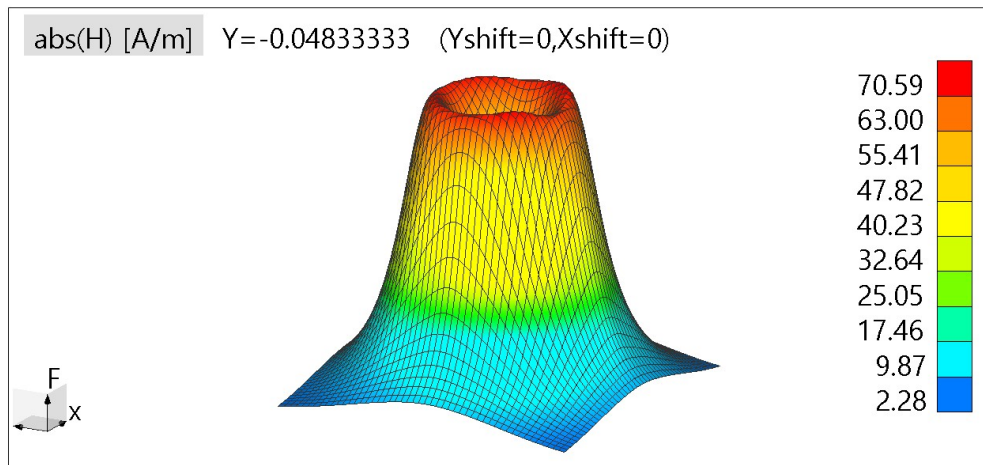


Figure 4.4: Coil-array IPT structure.

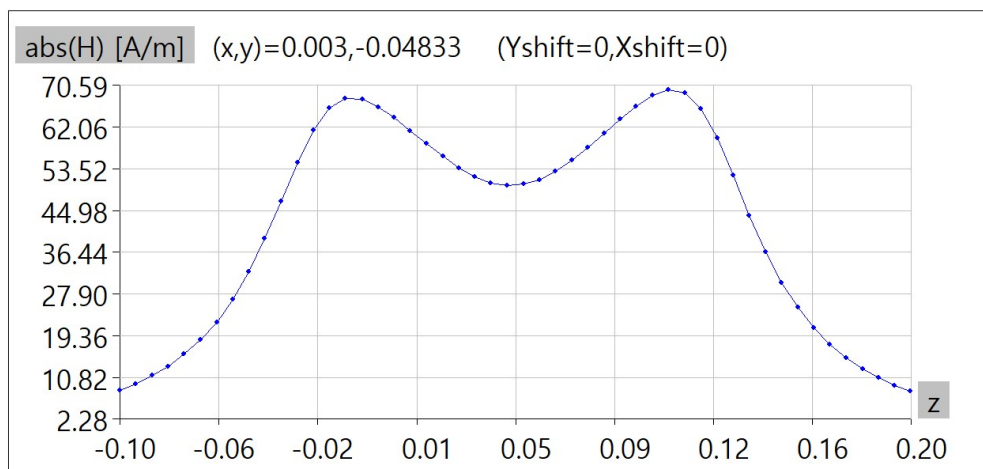


Figure 4.5: Coil-array IPT structure.

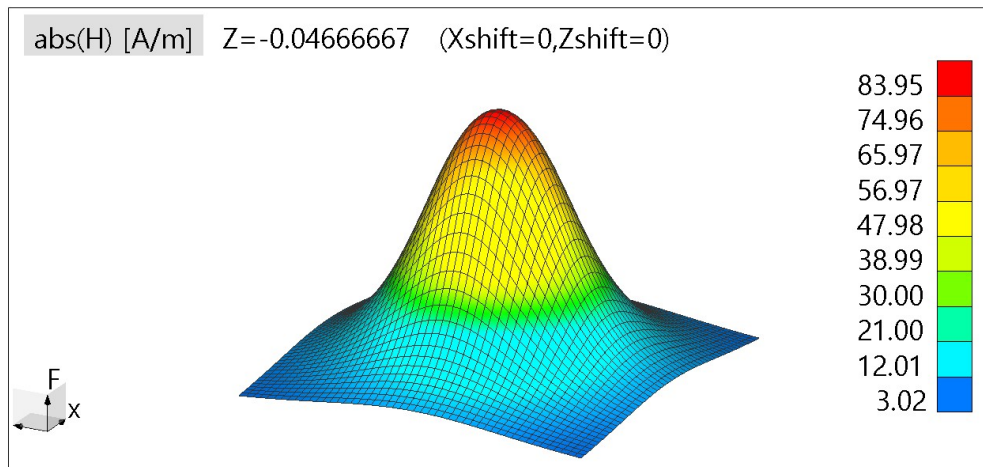


Figure 4.6: Coil-array IPT structure.

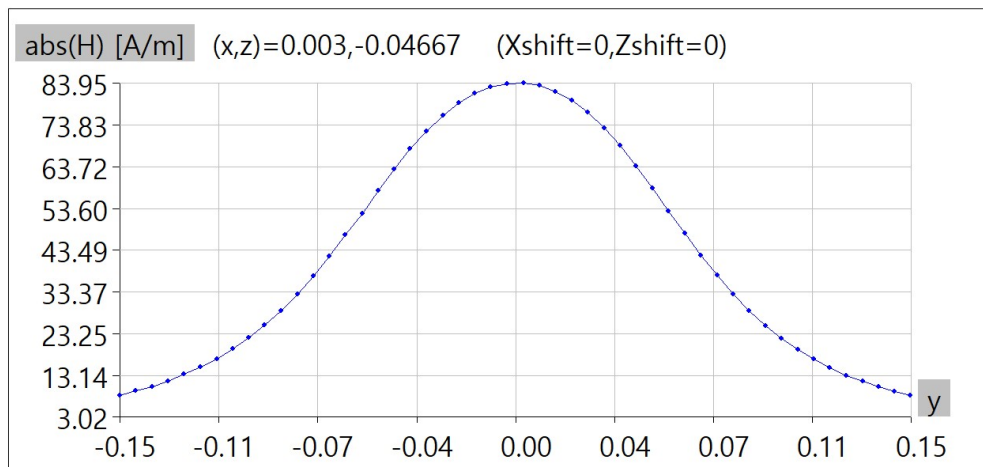


Figure 4.7: Coil-array IPT structure.



| Parameters             |   | Inner coil (Tx) | Outer coil (Rx) |
|------------------------|---|-----------------|-----------------|
| Diameter               |   | 100mm           | 160mm           |
| Number of coils        |   | 5               | 10              |
| Material               |   | Litz wire (2mm) | Litz wire (2mm) |
| 200kHz                 | Q | 207             | 206.25          |
|                        | L | 125.01 $\mu$ H  | 241.03 $\mu$ H  |
| Position of inner coil |   | center          |                 |
| $L_s$                  |   | 240.65 $\mu$ H  |                 |
| $M$                    |   | 6.8923          |                 |
| $k$                    |   | 0.0397          |                 |
| $kQ$                   |   | 8.2007          |                 |
| $\eta_{max}$           |   | 78.41%          |                 |

Figure 4.8: Coil-array IPT structure.

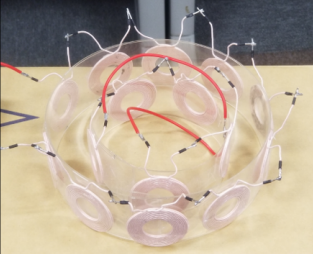
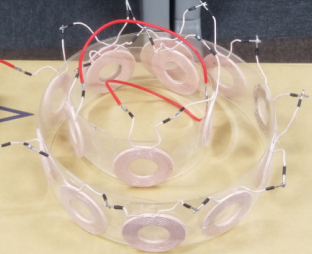
| Number of outer coils   |        | Number of inner coils  |         |
|---|--------|--|---------|
| 10  |        | 5  |         |
|  |        |  |         |
| $M$   | 4.2371 | $M$  | 8.9941  |
| $k$   | 0.0428 | $k$  | 0.0909  |
| $kQ$  | 7.5365 | $kQ$   | 15.9979 |
| $\eta_{max}$  | 76.75% | $\eta_{max}$   | 88.26%  |

Figure 4.9: Coil-array IPT structure.

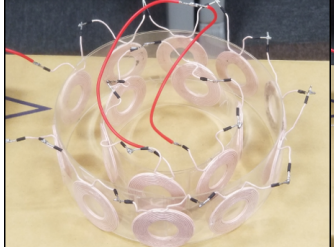
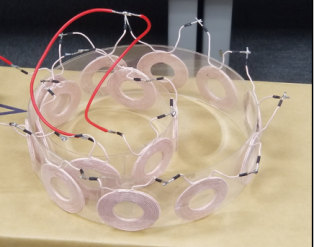
| <b>Number of outer coils</b>  | <b>Number of inner coils</b>   |
|---|--|
| 10  | 6  |
|  |  |
| $M$   | 4.7709   |
| $k$   | 0.0446   |
| $kQ$  | 7.6436   |
| $\eta_{max}$  | 77.03%   |
| $M$   | 13.4385  |
| $k$   | 0.1255   |
| $kQ$  | 21.5303  |
| $\eta_{max}$  | 91.13%   |

Figure 4.10: Coil-array IPT structure.

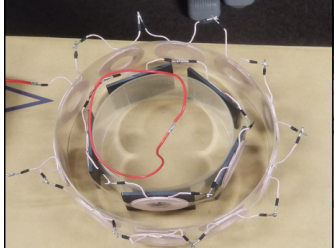
| <b>Number of outer coils</b>  | <b>Number of inner coils</b>   |
|---|--|
| 10  | 5  |
|  |  |
| $M$   | 8.3363   |
| $k$   | 0.0629   |
| $kQ$  | 12.2445  |
| $\eta_{max}$  | 84.95%   |
| $M$   | 5.8093   |
| $k$   | 0.0435   |
| $kQ$  | 8.3768   |
| $\eta_{max}$  | 78.81%   |

Figure 4.11: Coil-array IPT structure.

Table 4.1: Maximum power transfer efficiency.

| Shift                            | Numbers of coiL (Outer - Inner) | Both coils with ferrite | Both coils without ferrite | Outer coils without ferrite, inner coils with ferrite |
|----------------------------------|---------------------------------|-------------------------|----------------------------|---|
| Inner coil in the center         | 10 - 5                          | 78.41%                  | 76.75%                     | 84.95%  |
|                                  | 10 - 6                          |                         | 77.03%                     |   |
| Inner coil close to the one side | 10 - 5                          |                         | 88.26%                     | 78.80%  |
|                                  | 10 - 6                          |                         | 91.13%                     |   |

## 4.1 Simulation evaluation

### 4.1.1 Simulation evaluation

## 4.2 Coil array WPT in the air

- When we increase the number of inner coils, the maximum PTE (Power transfer efficiency) will increase.
- If the numbers of outer and inner coils are the same, when outer coils without ferrite and inner coils with ferrite, we can get the maximum PTE.
- When there is no ferrite outside the inner coil, the PTE will increase if the inner coil deviates from the middle, and vice versa.

## 4.3 Coil array WPT under seawater

# **5 Conclusion**

L

## **5.1 Future works**

# Acknowledgements

First of all, I would like to thank my supervisor, Professor Minoru Okada. Professor Okada is kind, knowledgeable, and rigorous in scientific attitude. Thank him for giving me an opportunity to study in Japan and let me do wireless power transfer research that I am interested in. He has continued to help me during my three years of study and life. At the same time, I would like to thank Professor Yuichi Hayashi for my research advice and guidance, so that I have a deeper understanding of the weak research environment. With his help, Which greatly improved my research.

Then I would like to thank Associate Professor Takeshi Higashino and Assistant Professor Duong Quang Thang. With their help, they have made me better understand the knowledge of wireless power transfer and wireless communication, and they have helped me overcome the difficulties in professional understanding and helped me complete this topic. Thank them very much. Here, I would also like to thank Assistant Professor Chen Na for her continuous help and encouragement in my studies, so that I have a better understanding of the field of communication.

I would also like to thank the members, staff, and seniors of the Network Systems Laboratory for their companionship in the study and life. We studied together and played together, and established a strong friendship together. Thank you to the international students who have helped me while studying abroad. Thank you for your kindness to me.

Finally, I would like to thank my family for their support of studying abroad, let me choose the knowledge I like, and always provide me with abundant financial support.

Thank you all for your kind help again.

# References

- [1] Orekan, T., Zhang, P.: Underwater Wireless Power Transfer—Smart Ocean Energy Converters. Springer Briefs in Energy. Springer, Cham (2019)
- [2] Nayyar, Anand & Balas, Valentina. (2019). Analysis of Simulation Tools for Underwater Sensor Networks (UWSNs): Proceedings of ICICC 2018, Volume 1. 10.1007978-981-13-2324-9\_17.
- [3] Chun T. Rim, Chris Mi: Wireless Power Transfer for Electric Vehicles and Mobile Devices, First Edition. John Wiley & Sons, (2017)
- [4] Song, B., Wang, Y., Zhang, K., & Mao, Z. (2018). Research on wireless power transfer system for Torpedo autonomous underwater vehicles. Advances in Mechanical Engineering.
- [5] Wang, Y.; Song, B.; Mao, Z. Application of Shielding Coils in Underwater Wireless Power Transfer Systems. J. Mar. Sci. Eng. 2019, 7, 267.